

Fabrication and characterization of $\text{SmO}_{0.7}\text{F}_{0.2}\text{FeAs}$ bulk with a transition temperature of 56.5 K

LIU Zhiyong^a, MA Lin^a, ZHAO Junjing^{b, c}, YAN Binjie^a, and SUO Hongli^a^a College of Materials Science and Engineering, Beijing University of Technology, Beijing 100022, China^b Department of Physics, University of Illinois at Chicago, Chicago, IL 60607, America^c Materials Science Division, Argonne National Laboratory, Argonne, IL 60439, America

Received 21 October 2010; received in revised form 24 December 2010; accepted 10 January 2011

© The Nonferrous Metals Society of China and Springer-Verlag Berlin Heidelberg 2011

Abstract

The superconductivity of iron-based superconductor $\text{SmO}_{0.7}\text{F}_{0.2}\text{FeAs}$ was investigated. The $\text{SmO}_{0.7}\text{F}_{0.2}\text{FeAs}$ sample was prepared by the two-step solid-state reaction method. The onset resistivity transition temperature is as high as 56.5 K. X-ray diffraction (XRD) results show that the lattice parameters a and c are 0.39261 and 0.84751 nm, respectively. Furthermore, the global J_c was more than $2.3 \times 10^5 \text{ A/cm}^2$ at $T = 10 \text{ K}$ and $H = 9 \text{ T}$, which was calculated by the formula of $J_c = 20\Delta M/[a(1 - a/(3b))]$. The upper critical fields, $H_{c2} \approx 256 \text{ T}$ ($T = 0 \text{ K}$), was determined according to the Werthamer-Helfand-Hohenberg formula, indicating that the $\text{SmO}_{0.7}\text{F}_{0.2}\text{FeAs}$ was a superconductor with a very promising application.

Keywords: iron-based superconductor; $\text{SmO}_{0.7}\text{F}_{0.2}\text{FeAs}$; solid-state reaction

1. Introduction

Since the discovery of layered copper oxide superconductors [1-2], some researches have been focused on exploring higher T_c materials. MgB_2 , which was discovered in the early 2001 [3-4], aroused people to search for new superconductors due to its unique performance compared with the traditional low-temperature and high-temperature oxide conductors. Recently, superconductivity in iron and nickel-based layered quaternary compounds has been reported: They were LaOFeP ($T_c=4 \text{ K}$) [5], LaONiP ($T_c=3 \text{ K}$) [6], and LaOFeAs ($T_c=26 \text{ K}$) [7]. Moreover, the T_c of iron-based superconductors has been greatly improved. It has been increased as high as 50 K in $\text{ReO}_{1-x}\text{F}_x\text{FeAs}$, with the replacement of La by other rare-earth elements such as Pr, Nd, Sm, Ce, and Gd [8-16]. These quaternary superconductors have the tetragonal layered ZrCuSiAs structure, $P4/nmm$ symmetry, and alternating FeAs and ReO layers [7-8, 17], similar to cuprates. In this paper, we reported the preparation and superconductivity of $\text{SmO}_{0.7}\text{F}_{0.2}\text{FeAs}$, whose onset resistivity transition temperature is as high as 56.5 K.

2. Sample preparation

The Sm chip, As, Fe, and Fe_2O_3 powders were all with

purity better than 99.99%; the purity of FeF_3 was 97%. The precursor SmAs was home-synthesized by reacting mixtures of Sm chips and As powder in an evacuated quartz tube (the vacuum was better than 10^{-5} Pa) at $600 \text{ }^\circ\text{C}$ for 5 h, then followed by heating to $900 \text{ }^\circ\text{C}$ holding for 20 h. The excess of 1 wt.% was added to compensate for the loss of As by volatilization [14].

The $\text{SmO}_{0.7}\text{F}_{0.2}\text{FeAs}$ sample was prepared by the two-step solid-state reaction method with the starting materials Fe, Fe_2O_3 , FeF_3 , and the obtained SmAs powders with the ratio being 14:7:2:30. The stoichiometric mixture of the starting materials was ground thoroughly and pressed into pellets. The obtained pellets were sintered in an evacuated quartz tube at 900°C for 5h, then 1200°C for 40 h, and then the samples were furnace-cooled to room temperature. The vacuum in the evacuated quartz tube was at the order of 10^{-5} Pa .

The phase purity and structural identification were characterized by powder X-ray diffraction (XRD) analysis on an MXP18A-HF type diffractometer with $\text{Cu K}\alpha$ radiation from 20° to 80° with a step of 0.02° . The resistivity of the sample was measured by the standard four-probe method from 30 to 300 K. The DC magnetization was measured using a Quantum Design MPMS XL-1 system.

3. Results and discussion

Fig. 1 shows the comparison of XRD patterns for both nominal SmOFeAs and SmO_{0.7}F_{0.2}FeAs samples; the nominal SmOFeAs sample was also synthesized by the two-step solid-state reaction method. The XRD results indicate that the main phase of non-doped and F-doped samples have the same structure with slight impurity phases. The major impurity phases such as unreacted SmAs are observed in our present samples, in addition to slight impurity phase of SmOF in F-doped SmO_{0.7}F_{0.2}FeAs sample. The impurity phases have been identified to be some by-products, which do not have superconductivity. The lattice parameters for the nominal SmO_{0.7}F_{0.2}FeAs are $a = 0.39261$ nm, $c = 0.84751$ nm, which are smaller than those of nominal SmO_{0.7}F_{0.3}FeAs in Ref. [18]. For the SmO_{0.7}F_{0.2}FeAs, due to the lack of F, its lattice constants are even smaller.

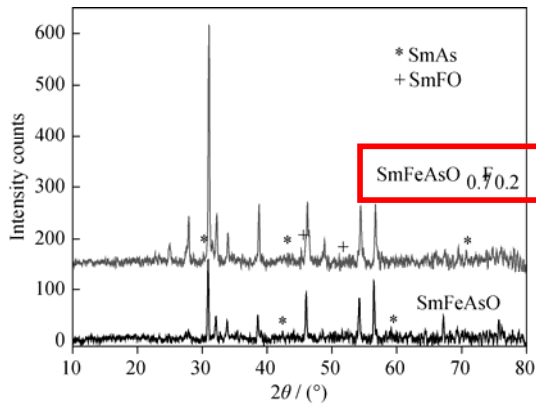


Fig. 1. Typical XRD patterns for the non-doping SmOFeAs and F-doped SmO_{0.7}F_{0.2}FeAs samples.

In Fig. 2, it can be seen from the inset that a clear superconducting onset transition (T_c (onset)) occurred at 56.5 K, and a zero resistivity transition (T_c (zero)) at 53 K for the nominal SmO_{0.7}F_{0.2}FeAs was obtained, which is about 1.5 K higher than that of Ref. [12]. This may be due to the smaller

lattice constant of SmO_{0.7}F_{0.2}FeAs sample described above. The SmO_{0.7}F_{0.2}FeAs sample has a metallic behavior when the temperature goes up to 300 K. The residual resistivity ratio RRR = $\rho_{(300\text{ K})}/\rho_{(55\text{ K})}$ was about 5.3, and the transition width ΔT is about 3 K, which shows that the SmO_{0.7}F_{0.2}FeAs sample has a high purity, but the fish tail indicate the existence of some non-superconducting impurities.

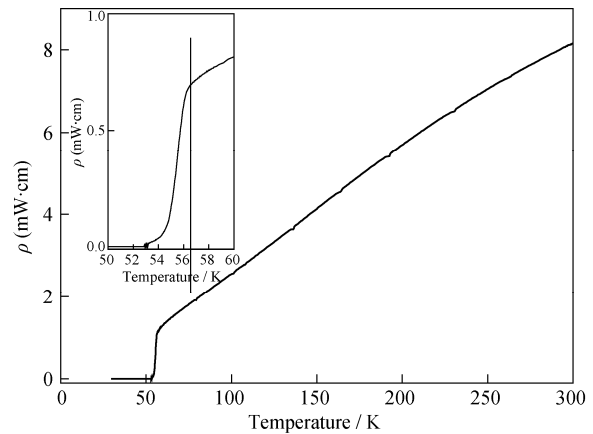


Fig. 2. Temperature dependence of resistivity for the nominal SmO_{0.7}F_{0.2}FeAs sample. The inset shows a clearer superconducting transition image.

For an experimental cycle, the SmO_{0.7}F_{0.2}FeAs sample was cooled down to 30 K in zero field cooling (ZFC), and the data were gathered when warmed in an applied field, then cooled again under an applied field (field cooling, FC), and measured when warming up. The DC-susceptibility data (measured under a magnetic field of 1591.5 A/m) of the SmO_{0.7}F_{0.2}FeAs are shown in Fig. 3. The magnetic onset T_c for the SmO_{0.7}F_{0.2}FeAs sample is at 56.5 K, which is consistent with the resistivity result. The existence of a superconducting phase is confirmed by the Meissner effect by cooling it in a magnetic field while the resistance goes to zero.

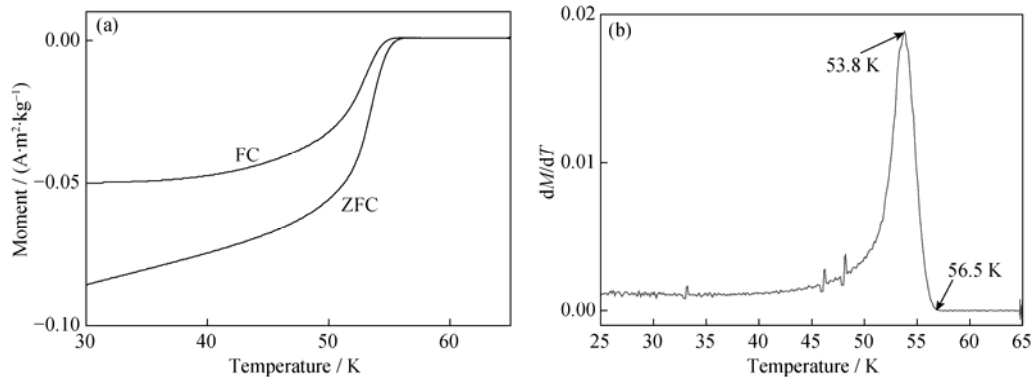


Fig. 3. Temperature dependence of the DC-susceptibility (a) and the differential ZFC curve (b) for the nominal SmO_{0.7}F_{0.2}FeAs

sample.

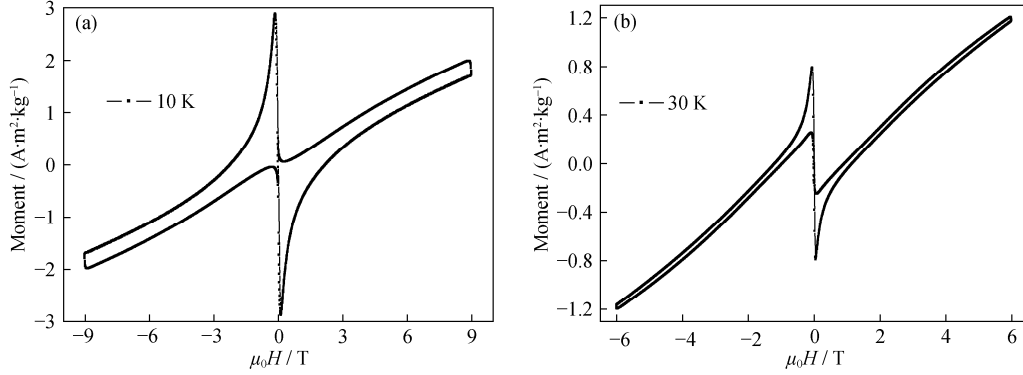


Fig. 4. M - H loops at various temperatures for $\text{SmO}_{0.7}\text{F}_{0.2}\text{FeAs}$ sample at 10 K (a) and 30 K (b).

Figs. 4(a) and 4(b) show the typical M - H hysteresis loops of $\text{SmO}_{0.7}\text{F}_{0.2}\text{FeAs}$ at 10 and 30 K, respectively. The gap in the loop drops dramatically in the low-field region with increased applied field, but it rapidly reaches a slowly decreasing state over a wide range of applied magnetic field. The rapid decrease in the wide hysteresis loop is a typical abnormal behavior for granular superconductors, since the weak superconductivity in the grain boundaries is extremely sensitive to the magnetic field. The global J_c of the samples is calculated on the basis of the following formula:

$$J_c = \frac{20\Delta M}{a(1 - a/(3b))}$$

where ΔM is the height of the magnetization loop and a and b are the dimensions of the sample perpendicular to the magnetic field with $a < b$. Fig. 5 presents the J_c - H curves of $\text{SmO}_{0.7}\text{F}_{0.2}\text{FeAs}$ at 10 and 30 K, respectively. It shows that J_c drops drastically in the low-field region with the increase of the applied field from 0 to 3 T, which illustrates that the grain boundaries are a weak-link behavior for the granular $\text{SmO}_{0.7}\text{F}_{0.2}\text{FeAs}$ sample, but J_c rapidly reduces and then becomes stable over a wide range of applied magnetic field from 3 T to 9 T. The J_c of $\text{SmO}_{0.7}\text{F}_{0.2}\text{FeAs}$ is more than $2.3 \times 10^5 \text{ A}/\text{cm}^2$ at 10 K and has a very weak dependence on the field, which shows that $\text{SmO}_{0.7}\text{F}_{0.2}\text{FeAs}$ has a fairly large pinning force in the grain. But at high temperature, J_c drops drastically with the increase of the applied field. This shows that the magnetic flux pinning ability has been badly damaged in the sample at the high temperature.

Fig. 6 shows the temperature dependence of electrical resistivity of the superconducting $\text{SmO}_{0.7}\text{F}_{0.2}\text{FeAs}$ sample at different magnetic fields. An empirical criterion for the onset of superconductivity at a given applied field would be the deviation from the apparent linear behavior of the normal-state resistivity (ρ_n). Using this criterion, we define

transition temperatures T_c^{on} , T_c^{mid} , and T_c^{10} corresponding to 90%, 50%, and 10% of ρ_n , respectively. With the increase of the magnetic field from 0 to 9 T, both the onset transition

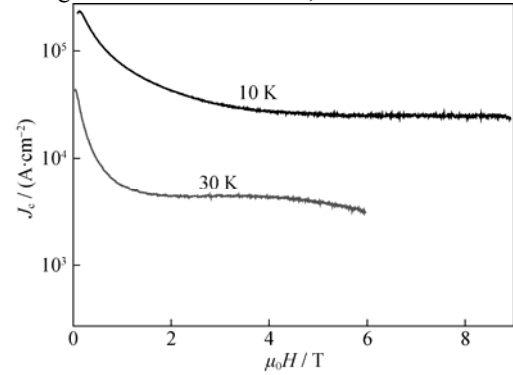


Fig. 5. J_c - H curves for the $\text{SmO}_{0.7}\text{F}_{0.2}\text{FeAs}$ sample at 10 and 30 K.

point (T_c^{on}) and the zero-resistance point shift toward lower temperature, with T_c^{on} by 2 K, while the latter by 10 K. This is understandable since the latter is determined by the weak links between the grains and the vortex flow of magnetic flux lines, while the former is controlled by the upper critical field of the individual grains. The temperature dependence of H_{c2} , H_{irr} , and H_{peak} determined from the 90%, 50%, and 10% of ρ_n criteria is shown in Fig. 7. The values of $(dH_{c2}/dT)_{T_c}$ for 10%, 50%, and 90% of ρ_n , are -1.3 , -2.4 , -4.1 TK^{-1} , respectively. It needs to be mentioned that the slope $(dH_{c2}/dT)_{T_c}$ determined with different criteria is a linear function of the curve shown in Fig. 7. At low temperatures, well below T_c , where the flux flow dominates resistivity, an empirical relation $\rho/\rho_n = H/H_c$ has been shown. Using the conventional single-band Werthamer-Helfand-Hohenberg (WHH) theory:

$$H_{c2}^{WHH}(0) = 0.693T_c(dH_{c2}/dT)_{T_c},$$

One can estimate $H_{c2}(0)$ from the slope of the $H_{c2}(T)$ curve at $T = T_c$. For the 90% ρ_n criterion ($T_c = 56$ K), $H_{c2}(0)$ is about 256 T. $H_{c2}(0)$ can be estimated from the Ginzburg-Landau (G-L) mean-field theory. According to this theory, $H_{c2} = \phi_0/2\pi\xi^2$ and $\xi^2 \propto (1+t^2)/(1-t^2)$, where ϕ_0 is the flux quantum, ξ is the coherence length, and $t = T/T_c$ is the reduced temperature. From the above relation, one obtains

$$H_{c2}(T) = H_{c2}(0)(1-t^2)/(1+t^2).$$

The value of $H_{c2}(0)$ obtained from the G-L equation is about 203 T for the 90% ρ_n criterion. Apparently, the estimated values of the upper critical fields obtained from the WHH theory (256 T) and the G-L theory (203 T) are much higher than the BCS paramagnetic limit $H_p^{BCS} = 1.84T_c$ in the weak-coupling regime. However, the BCS model underestimates H_p in the presence of strong e-ph coupling. In such a case, the actual Pauli paramagnetic limit is $H_p \approx (1 + \lambda)H_p^{BCS}$, where λ is the e-ph coupling constant. Using the value of $\lambda \sim 1.5$ as estimated from the $\rho(T)$ curve of a $\text{PrO}_{0.6}\text{F}_{0.12}\text{FeAs}$ sample [19], the paramagnetic limit H_p increases to ~ 240 T. Such a high value of zero-temperature upper critical field is comparable with that observed in cuprate superconductors.

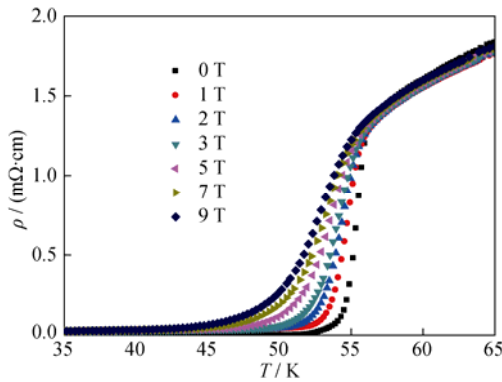


Fig. 6. Temperature dependence of resistivity for the $\text{SmO}_{0.7}\text{F}_{0.2}\text{FeAs}$ sample in the low-temperature region under different fields.

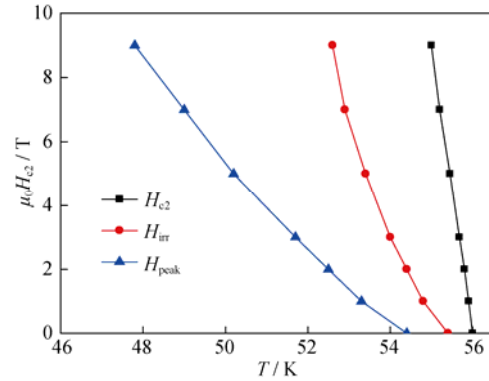


Fig. 7. Upper critical fields H_{c2} versus temperature for the $\text{SmO}_{0.7}\text{F}_{0.2}\text{FeAs}$ sample as determined from the 90%, 50%, and 10% criteria of the normal-state resistivity, respectively.

4. Conclusion

The F-doped $\text{SmO}_{0.7}\text{F}_{0.2}\text{FeAs}$ was prepared by the two-step solid-state reaction method. The optimal nominal $\text{SmO}_{0.7}\text{F}_{0.2}\text{FeAs}$ is found to have the highest T_c at 56.5 K (onset) in the Sm-system. The XRD results indicate a clear shrinkage of lattice parameters in the F-doping sample compared with that of the undoped one. The electrical resistivity and the DC-susceptibility (measured under a magnetic field of 1591.5 A/m) of the $\text{SmO}_{0.7}\text{F}_{0.2}\text{FeAs}$ show that a clear superconducting onset transition ($T_{c(\text{onset})}$) occurred at 56.5 K and a zero resistivity transition ($T_{c(\text{zero})}$) at 53 K for the nominal $\text{SmO}_{0.7}\text{F}_{0.2}\text{FeAs}$, which is the optimal T_c in this Sm-system. The transition width ΔT is about 3 K, meaning that our sample has a high quality. The typical M - H hysteresis loops at 10 K show that the rapid decrease in the wide range of the hysteresis loop is not a typical behavior of granular superconductors since the weak superconductivity in the grain boundaries is extremely sensitive to the magnetic field. The global J_c was calculated on the basis of $J_c = 20\Delta M/[a(1 - a/(3b))]$. At 10 K, the J_c of $\text{SmO}_{0.7}\text{F}_{0.2}\text{FeAs}$ is more than 2.3×10^5 A/cm², which has a very weak dependence on the field, showing that $\text{SmO}_{0.7}\text{F}_{0.2}\text{FeAs}$ has a fairly large pinning force in the grain. According to the conventional single-band Werthamer-Helfand-Hohenberg (WHH) theory, $H_{c2}(0)$ is about 256 T.

Acknowledgments

The authors are very grateful to NI Baorong, Professor from Fukuoka Institute of Technology, Japan, for his guidance and assistance. This work is financially supported by the National Basic Research Program of China (No. 2006CB601005), the National High Technology Research

and Development Program of China (No. 2009AA032401), the National Natural Science Foundation of China (Nos. 50771003 and 50802004), the Beijing Municipal Natural Science Foundation (No. 2092006), and the Program for New Century Excellent Talents in University of Ministry of Education of China (No. 39009001201002).

References

- [1] Bednorz J.G. and Mueller K.A., Possible high T_C superconductivity in the Ba-La-Cu-O system, *Z. Phys.*, 1986, **B64** (2): 189.
- [2] Chu C.W., Hor P.H., Meng R.L., Gao L., Huang Z.J., and Wang Y.Q., Evidence for superconductivity above 40 K in the La-Ba-Cu-O compound system, *Phys. Rev. Lett.*, 1987, **58**: 405.
- [3] Nagamatsu J., Nakagawa N., Muranaka T., Zenitani Y., and Akimitsu J., Superconductivity at 39 K in magnesium diboride, *Nature*, 2001, **410**: 63.
- [4] Flükiger R., Suo H.L., Musolino N., Beneduce C., and Lezza P., Superconducting properties of MgB₂ tapes and wires, *Phys. C*, 2003, **385**: 286.
- [5] Kamihara Y., Hiramatsu H., Hirano M., and Hosono H., Abstracts in physical inorganic chemistry iron-based layered superconductor: LaOFeP, *J. Am. Chem. Soc.*, 2006 **128**: 10012.
- [6] Watanabe T., Yanagi H., Kamiya T., Hirano M., and Hosono H., Nickel-based oxyphosphide superconductor with a layered crystal structure, LaNiOP, *Inorg. Chem.*, 2007, **46**: 7719.
- [7] Kamihara Y., Watanabe T., Hirano M., and Hosono H., Iron-based layered superconductor La[O_{1-x}F_x]FeAs ($x = 0.05-0.12$) with $T_C = 26$ K, *J. Am. Chem. Soc.*, 2008, **130**: 3296.
- [8] Chen X. H., Wu T., Wu G., Chen H., and Fang D. F., Superconductivity at 43 K in Samarium-arsenide oxides SmFeAsO_{1-x}F_x, *Nature*, 2008, **453**: 761.
- [9] Chen G.F., Li Z., Wu D., Li G., and Wang N.L., Superconducting properties of the Fe-based layered superconductor LaFeAsO_{0.9}F_{0.1}, *Phys. Rev. Lett.*, 2008, **101**: 057007.
- [10] Ren Z.A., Yang J., Lu W., Yi W., and Zhao Z.X., Superconductivity at 52 K in iron-based F-doped layered quaternary compound Pr[O_{1-x}F_x]FeAs, *Mater. Res. Innov.*, 2008, **12** (3): 105.
- [11] Ren Z.A., Yang J., Lu W., Yi W., Zhou F., and Zhao Z.X., Superconductivity in iron-based F-doped layered quaternary compound Nd[O_{1-x}F_x]FeAs, *Europhys. Lett.*, 2008, **82**: 57002.
- [12] Ren Z.A., Lu W., Yang J., and Zhao Z.X., Superconductivity at 55K in iron-based F-doped layered quaternary compound Sm[O_{1-x}F_x]FeAs, *Chin. Phys. Lett.* 2008, **25**: 2215.
- [13] Chen G.F., Li Z., Wu D., Li G., Luo J.L., and Wang N.L., Superconductivity at 41K and its competition with spin-density- wave instability in layered CeO_{1-x}F_xFeAs, *Phys Rev Lett.* 2008, **100**: 247002.
- [14] Yang J., Li Z.C., Lu W., Yi W., and Zhao Z.X., Superconductivity at 53.5 K in GdFeAsO_{1- δ} , *Supercond. Sci. Technol.*, 2008, **21**: 082001.
- [15] Gao Z.S., Wang L., Ma Y.W., and Wen H.H., Superconducting properties of granular SmFeAsO_{1-x}F_x wires with $T = 52$ K prepared by the powder-in-tube method, *Supercond. Sci. Technol.*, 2008, **21**: 112001.
- [16] Wei Z., L H.O., and Ruan K.Q., Superconductivity at 57.3 K in La-doped iron-based layered compound Sm_{0.95}La_{0.05}O_{0.85}-F_{0.15}FeAs, *J. Supercond. Nov. Magn.*, 2008, **21**: 213.
- [17] Martinelli A., Ferretti M., Putti M., and Siri A.S., Synthesis, crystal structure, microstructure, transport and magnetic properties of SmFeAsO and SmFeAs(O_{0.93}F_{0.07}), *Supercond. Sci. Technol.*, 2008, **21**: 095017.
- [18] Wang L., Gao Z.S., Qi Y.P., and Ma Y.W., Structural and critical current properties in polycrystalline SmFeAsO_{1-x}F_x, *Supercond. Sci. Technol.*, 2009, **22**: 015019.
- [19] Bhoi D., Manda P., and Choudhury P., Resistivity saturation in PrFeAsO_{1-x}F_y superconductor: evidence of strong electron-phonon coupling, *Supercond. Sci. Technol.*, 2008, **21**: 125021.